Journal of Crystal Growth 350 (2012) 27–32

Contents lists available at SciVerse ScienceDirect

Journal of Crystal Growth

journal homepage: www.elsevier.com/locate/jcrysgro

Structural and optical studies of thick freestanding GaN films deposited by Hydride vapor phase epitaxy

J.A. Freitas Jr.[a,*], M.A. Mastro[a], E.R. Glaser[a], N.Y. Garces[b,1], S.K. Lee[c], J.H. Chung[c], D.K. Oh[d], K.B. Shim[d]

[a] Naval Research Laboratory, Washington DC 20375, USA
[b] Global Strategies Group, North America Crofton, MD 21114, USA
[c] Unimo Photron, Seoul 137-791, Republic of Korea
[d] Hanyang University, Seoul 133-791, Republic of Korea

ARTICLE INFO

Available online 13 December 2011

Keywords:
A1. Emission
A1. Impurity
A2. Freestanding
A3. Grown from vapor
B1. Nitrides
B2. Semiconductors

ABSTRACT

Thick freestanding films or bulk GaN substrates with very low background impurity levels ($\leq 1\times10^{15}/cm^3$) and high crystalline quality are required for a number of electronic device applications. Low pressure chemical vapor and molecular beam epitaxy techniques can systematically deposit films with low residual impurity concentrations. However, their typical slow growth rate prevents their utilization for substrate growth. The hydride vapor phase epitaxy deposition technique can achieve hundreds of microns per hour growth rate, but these films have typically high free carrier concentration ($\geq 3\times10^{17}/cm^3$). It is crucial to verify if this method can reproducibly deliver thick freestanding GaN films of high crystalline quality with exceptionally low free carrier concentration. Low temperature photoluminescence and room temperature Raman scattering experiments carried out on a number of samples indicate that they have high crystalline quality and uncommonly low donor background levels. Reduced concentration of uncompensated shallow donors verified by low temperature electron paramagnetic resonance was confirmed by detailed high sensitive SIMS analyses. In addition, it was verified by X-ray diffraction analysis that relatively low dislocation densities can be achieved.

Published by Elsevier B.V.

1. Introduction

The high free-electron concentration in unintentionally doped GaN substrates is desirable for optoelectronic device fabrication, but is deleterious to the high-frequency response of high-electron mobility transistors and high voltage Schottky diodes. Impurities such as iron have been added during growth to introduce deep compensation levels, which reduces the room temperature free-electron concentration [1]. However, such an approach introduces structural defects and reduces the thermal conductivity of GaN, which is a limitation to the thermal management of electronic devices. Therefore, the realization of high-performance GaN-based devices depends on the commercial availability of large-area high-quality substrates with controlled carrier type and concentration.

It has been demonstrated that the metal organic chemical vapor deposition (MOCVD) process can deposit thick stress-free homoepitaxial film with room temperature net free electron concentration on the order of $2\times10^{15}/cm^3$, as verified by capacitance–voltage measurements performed at 30 °C [2]. Impurity trace analysis of this 14 μm thick film indicates that low background impurity levels were achieved, which is a basic requirement for high breakdown blocking layers in fast switches. This preliminary result is quite encouraging, but numerical calculation indicates that to achieve a 10 kV breakdown voltage, films with $1\times10^{15}/cm^3$ free carrier concentration must have thickness exceeding 50 μm [3]. These relatively large required film thicknesses make difficult the use of deposition techniques such as MOCVD, which has growth rates typically on the order of 2 μm/h. Therefore, a technique with higher growth rate such as hydride vapor phase epitaxy (HVPE), which can reach growth rates well above 100 μm/h, becomes a better option. A problem to address is the higher free carrier concentration of samples grown by HVPE, which are typically in the order of $\geq 3\times10^{17}/cm^3$.

In the present work, we use a combination of spectroscopic techniques to investigate the structural, optical, and electrical properties of thick (>1 mm) unintentionally doped freestanding GaN films grown by HVPE, to verify if this method can reproducibly yield high crystalline quality substrates with a low concentration of free carriers.

2. Growth and experimental techniques

Unintentionally doped GaN films with thicknesses ranging from ≤ 2 mm to ≥ 3 mm have been successfully deposited on

* Corresponding author.
E-mail address: jaime.freitas@nrl.navy.mil (J.A. Freitas Jr.).
[1] Residing at Naval Research Laboratory.

0022-0248/$ - see front matter Published by Elsevier B.V.
doi:10.1016/j.jcrysgro.2011.12.017

Report Documentation Page

Form Approved
OMB No. 0704-0188

1. REPORT DATE	2. REPORT TYPE	3. DATES COVERED
2012		**00-00-2012 to 00-00-2012**

4. TITLE AND SUBTITLE
Structural and optical studies of thick freestanding GaN films deposited by Hydride vapor phase epitaxy

5a. CONTRACT NUMBER
5b. GRANT NUMBER
5c. PROGRAM ELEMENT NUMBER

6. AUTHOR(S)

5d. PROJECT NUMBER
5e. TASK NUMBER
5f. WORK UNIT NUMBER

7. PERFORMING ORGANIZATION NAME(S) AND ADDRESS(ES)
Naval Research Laboratory,4555 Overlook Ave SW,Washington,DC,20375

8. PERFORMING ORGANIZATION REPORT NUMBER

9. SPONSORING/MONITORING AGENCY NAME(S) AND ADDRESS(ES)

10. SPONSOR/MONITOR'S ACRONYM(S)
11. SPONSOR/MONITOR'S REPORT NUMBER(S)

12. DISTRIBUTION/AVAILABILITY STATEMENT
Approved for public release; distribution unlimited

13. SUPPLEMENTARY NOTES

14. ABSTRACT

ThickfreestandingfilmsorbulkGaNsubstrateswithverylowbackgroundimpuritylevels(r1 1015/cm3) and highcrystallinequalityarerequiredforanumber ofelectronicdeviceapplications.Lowpressure chemicalvaporandmolecularbeamepitaxytechniques cansystematicallydepositfilmswithlowresidual impurityconcentrations.However,theirtypicalslowgrowthratepreventstheirutilizationforsubstrate growth. Thehydridevaporphaseepitaxydeposition techniquecanachievehundredsofmicronsperhour growth rate,butthesefilmshavetypicallyhighfreecarrierconcentration(Z3 1017/cm3). Itiscrucialto verify ifthismethodcanreproduciblydeliverthickfreestandingGaNfilmsofhighcrystallinequalitywith exceptionallylowfreecarrierconcentration.Lowtemperaturephotoluminescenceandroomtemperature Ramanscatteringexperimentscarriedoutonanumberofsamplesindicatethattheyhavehighcrystalline qualityanduncommonlylowdonorbackgroundlevels. Reduced concentrationofuncompensatedshallow donors verifiedbylowtemperatureelectronparamagneticresonancewasconfirmedbydetailedhigh sensitiveSIMSanalyses.Inaddition,itwasverifiedbyX-raydiffractionanalysisthatrelativelylow dislocationdensitiescanbeachieved.

15. SUBJECT TERMS

16. SECURITY CLASSIFICATION OF:			17. LIMITATION OF ABSTRACT	18. NUMBER OF PAGES	19a. NAME OF RESPONSIBLE PERSON
a. REPORT	b. ABSTRACT	c. THIS PAGE			
unclassified	**unclassified**	**unclassified**	**Same as Report (SAR)**	**6**	

sapphire substrates using the HVPE technique. A 2 in. *c*-plane sapphire substrate, previously cleaned to remove organic and inorganic contaminants, was placed on a vertical susceptor in a hot-wall reactor. The substrate temperature is raised under clean ammonia environment for surface nitridation. The Ga metal and the HCl gas are pre-reacted to form GaCl gas in the Source Zone, and transported by nitrogen carrier gas to the hot Growth Zone where reaction occurs with NH_3 and deposits GaN on the (0001) sapphire substrate at 1030 °C. For a V/III ratio from 15 to 50, a growth rate between 80 and 150 μm/h can be reproducibly achieved.

Secondary Ion Mass Spectrometry (SIMS) depth profiles were employed to trace the H, C, Si, and O impurity concentrations in the top 5 μm region of the samples. The hydrogen concentration is at the detection limit (DL) for all samples, while a uniform concentration of carbon around 1×10^{16} cm^{-3} is detected in most samples, except for samples #2 and #3, which have C level at the DL. Fig. 1a shows the SIMS profile of sample #1, which has 3.0×10^{16} cm^{-3} oxygen and 1.0×10^{15} cm^{-3} Si. Fig. 1b depicts the SIMS analysis of sample #2, which has a uniform concentration of 5–6 $\times 10^{16}$ cm^{-3} and 2–3 $\times 10^{16}$ cm^{-3} of oxygen and Si, respectively. As indicated in Table 1, sample #1 has the lowest

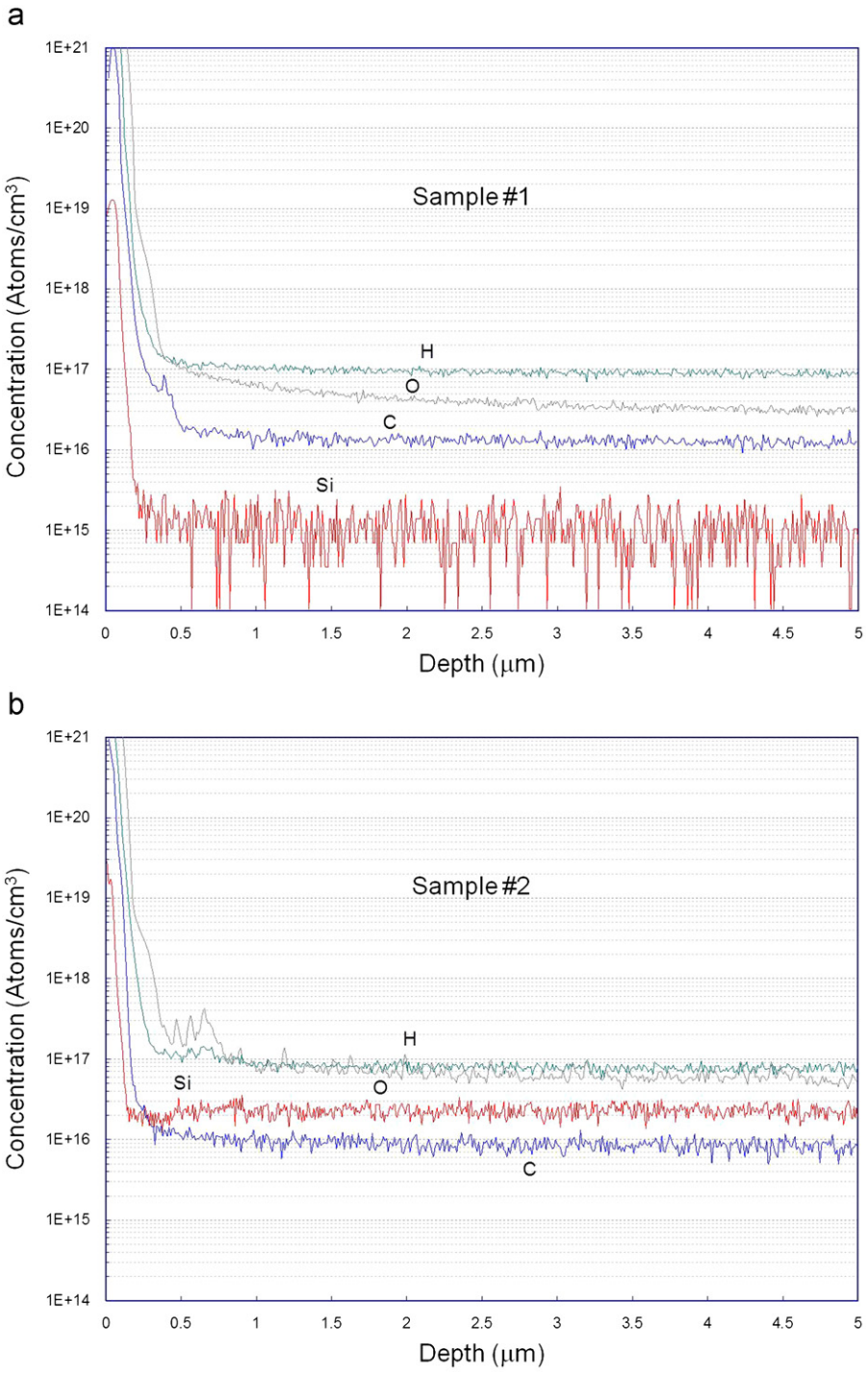

Fig. 1. (a) SIMS profile of S#1 and (b) SIMS profile of S#2.

Table 1
Summary of SIMS analyses for five bulk GaN samples investigated in this work.

Sample	O (cm^{-3})	Si (cm^{-3})	C (cm^{-3})	H (cm^{-3})
#1	3.0×10^{16}	1.0×10^{15}	$1–2\times10^{16}$	DL
#2	$5–6\times10^{16}$	$2–3\times10^{16}$	DL	DL
#3	4.0×10^{16}	$1–2\times10^{15}$	DL	DL
#4	3.0×10^{16}	$2–3\times10^{15}$	$1–2\times10^{16}$	DL
#5	4.0×10^{16}	$1–2\times10^{15}$	$1–2\times10^{16}$	DL
Detection limit	2.0×10^{16}	5×10^{14}	9×10^{15}	7×10^{16}

total concentration of donor background, while sample #2 has the highest. Note that the concentration of oxygen is more than one order of magnitude higher than that of Si. Despite that, this SIMS study shows that the impurity levels are considerably lower than values commonly reported for HPVE growth.

X-ray diffraction (XRD) and Raman scattering (RS) techniques were systematically employed to evaluate the structural properties of the samples. A Panalytical X-Ray diffraction (XRD) system with a Cu Kα source was used to measure the symmetric and skew-symmetric rocking curves. The micro-Raman spectra were acquired at room temperature with a 0.5 m single grating spectrometer equipped with a 1800 groves/mm grating and a liquid nitrogen cooled back-thinned/deep-depleted CCD, sensitive in the visible to near IR spectral range. The samples were illuminated with the 532 nm line of a solid-state laser, and typically a spot size of 1 μm and laser intensity of about 5 mW were employed for this experiment. Polarizers were used to control the laser polarization and select the scattering geometry.

The 5 K low- and high-resolution photoluminescence (PL) measurements were carried out to verify the dominant recombination processes to obtain insights on the optical and electronic properties of the samples. The luminescence was excited with the 325 nm line of a HeCd laser, and the laser excitation intensity was kept at ≤ 2 mW, using calibrated neutral density filters. The collected sample light emissions were dispersed by a double grating spectrometer fitted with 1800 groves/mm gratings. The spectra were acquired with a UV-sensitive GaAs photomultiplier tube coupled to a computer controlled photon counter.

The bulk GaN samples were also characterized by electron paramagnetic resonance (EPR) at 9.5 GHz. This technique has shown to be quite useful during the last several years as a way to chemically identify point defects such as transition metal impurities (e.g., Fe, Mn, Ni) [4,5] and irradiation-induced lattice defects [6,7] in epitaxial and bulk GaN. In addition, ESR has revealed Zeeman splitting *g*-value signatures of both shallow donor [8] and acceptor [9] centers in GaN. For our measurements, a conventional EPR spectrometer (Bruker EMX) was employed equipped with a liquid helium flow system for temperature control from 4.2 to 300 K [8]. Estimates of the spin concentrations for the various samples were made from single integration fits to the EPR line shapes and use of a well-calibrated P-doped Si standard.

3. Experimental results and discussions

X-ray diffraction measurements were carried out on the growth surface as well as the cleaved surface perpendicular to the *c*-plane surface. Analysis of the growth surface via a series of skew symmetric measurements extracted an edge dislocation density of $4.13\times10^{7}\,cm^{-2}$ and screw dislocation component density of $8.9\times10^{6}\,cm^{-2}$. Screw dislocations in *c*-axis GaN create a tilt of the lattice planes parallel to the surface and can be easily examined with symmetric (001) XRD rocking curves. Edge dislocations create a twist that can only be directly isolated in XRD with a grazing incidence beam, which is an experimentally challenging technique. Skew-symmetric XRD reflections taken at interplanar angles approaching grazing incidence can approximate this technique; however these rocking curves, e.g., the (302) reflection at 70.45° interplanar angle, also have contributions from the screw dislocations. Additionally, the peak broadening of the skew-symmetric XRD reflections is further complicated by interactions between the screw and edge dislocations as well as the limited correlation lengths common for GaN films grown on sapphire substrates. Recently, several models have been developed to extrapolate the contribution of tilt, twist, and correlation length in GaN films for a series of XRD symmetric and skew-symmetric ω-scans [10]. Lee et al. employs a peak fitting parameter, *n*, to assess the contribution of Lorentzian ($n=1$) to Gaussian ($n=2$) curve shape in the rocking curves [11]. A fit to the rocking curves as well as an extrapolation to 90° can be made with $\beta^{n}_{hkl}=(\beta_{\rm tilt}\cos X)^n+(\beta_{\rm twist}\sin X)^n+(1/L)^n/|K_{hkl}|^n$, where X is the interplanar angle, $|K_{hkl}|^n$ is the magnitude of the reciprocal scattering vector. Similar to the analysis of Lee et al., we found that the GaN bulk substrate had negligible correlation length and could be optimally fitted with a Gaussian curve shape. Overall the diffraction peaks were sharp indicating a low dislocation density. This low dislocation density combined with the apparent lack of distinct grains justified the use of the Dunn and Koch model for random distribution in a crystal, $D_{\rm B}=\beta^2/4.35b^2$, where b is the length of the Burgers vector.

An omega–2theta scan, depicted in Fig. 2a, confirmed that the major cleavage plane was *m*-plane. The small full-width at half-maximum (FWHM) of 0.087° observed near the top growth surface confirms the high crystalline quality at the near growth surface region.

The hexagonal phase of GaN, wurtzite structure belonging to the space group C^4_{6v}, has two molecules per unit cell. Group theory predicts eight zone-center optical modes, namely $1A_1$(TO), $1A_1$(LO), $2B_1$, $1E_1$(TO), $1E_1$(LO), and $2E_2$. The two B_1 modes are optically inactive, but all of the six allowed modes have been observed by Raman scattering spectroscopy. Raman scattering measurements performed along the direction perpendicular to the GaN (0001) plane or $z(xy,xy)\bar{z}$, only the E^1_2 (or E_2 low), E^2_2 (or E_2 high), and A_1(LO) should be observed. In particular, in the $z(x,x)\bar{z}$ and $z(y,y)\bar{z}$ geometries all three modes should be observed, while in the $z(x,y)\bar{z}$ or $z(y,x)\bar{z}$, only the E_2 modes should be detected [12]. These observations are highlighted in Fig. 3a and b for orientations $z(y,y)\bar{z}$, $x(z,z)\bar{x}$, and $x(y,y)\bar{x}$. The observed allowed phonons frequencies are 143.2 cm^{-1} (E^1_2), 568.1 cm^{-1} (E^2_2), 532.1 cm^{-1} ($1A_1$/TO), 735.2 cm^{-1} ($1A_1$/LO), 559.4 (E_1/TO), and 741.9 cm^{-1} (E_1/TO). The observation of small intensities of the non-allowed modes, which are forbidden in some of these geometries, could be attributed to internal reflections, small tilting of the samples, and/or surface irregularities (The pictures of sample S#4 included in Fig. 3a and b, show that the sample surfaces were not lapped or polished.) The small FWHM of the A_1(LO) phonon is consistent with low room-temperature free-carrier concentration [13,14]. A more detailed Raman scattering study is in progress.

The low-resolution PL spectra of five thick GaN samples at 5 K, covering the spectral range between 1.95 and 3.72 eV, are depicted in Fig. 4a. All spectra are dominated by an intense sharp line around 3.47 eV, represented by NBE (near band edge) emission, associated with the recombination processes involving the annihilation of free excitons and excitons bound to neutral shallow donors [15]. Also observed are three relatively weak bands at 2.25 eV, ~2.45 eV, and at 3.1 eV. The former is the well-known yellow band and the latter has been observed in carbon doped GaN films [16]. Similar spectra have been often observed in unintentionally doped (UID) GaN films characterized by high resistivity and large breakdown voltage [17]. Therefore, it is expected that these defects partially compensate the free carriers

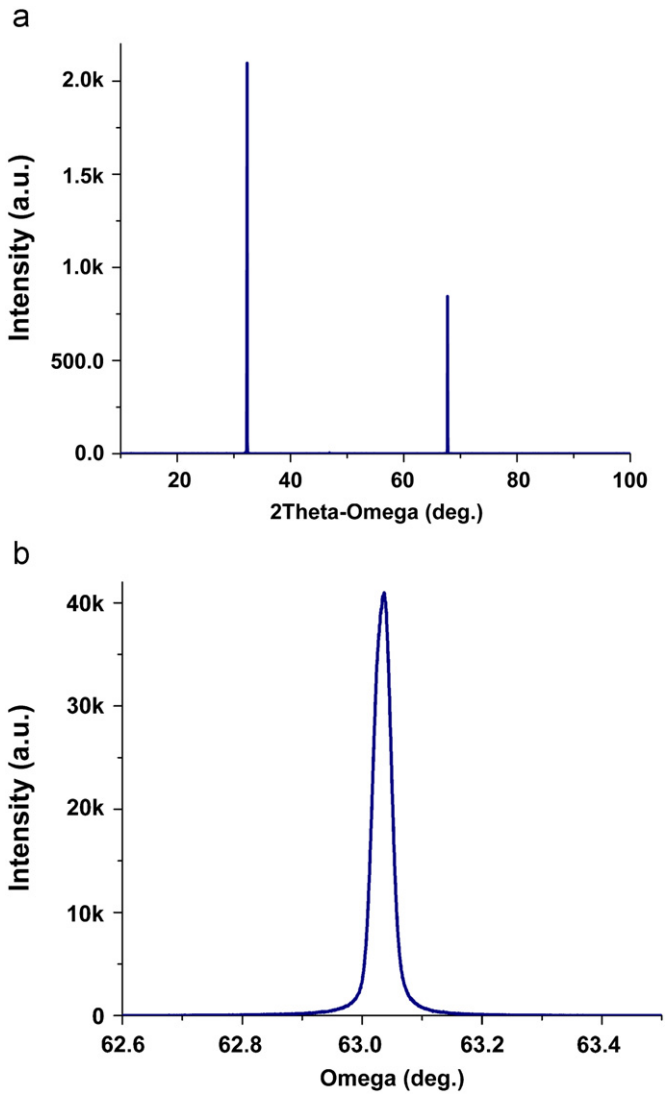

Fig. 2. (a) An omega–2theta XRD scan of the major cleavage plane displays the m-plane (10–10) and (20–20) reflections (sample S#4) and (b) XRD (20–20) omega rocking curve.

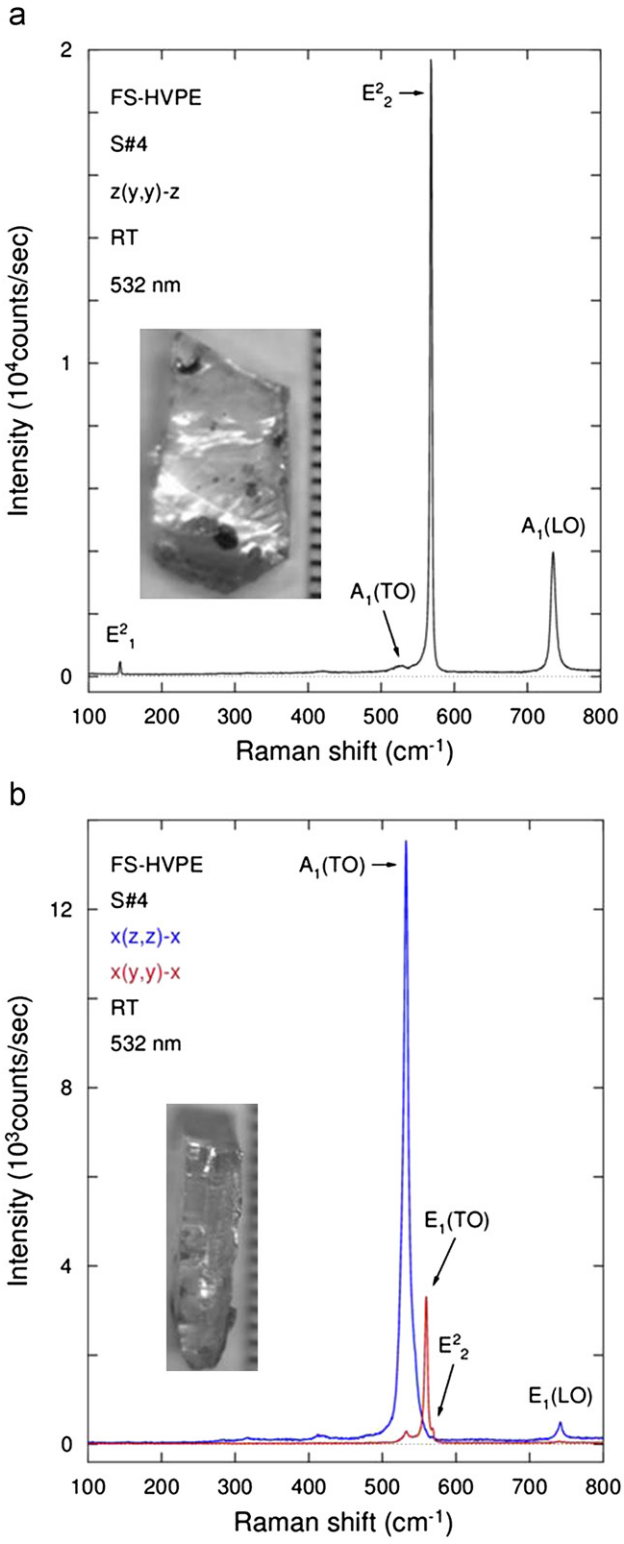

Fig. 3. (a) Raman scattering spectra measured at the basal plane of sample S#4 with the $z(y,y)\bar{z}$ geometry. Sample picture and scale in mm/division are included (b) Raman scattering spectra measured at the flat cross-section face of sample S#4 with the $x(z,z)\bar{x}$ and $x(y,y)\bar{x}$ geometries. Sample picture and scale in mm/division are included.

associated with the unintentional oxygen and silicon shallow donors in GaN. Also observed in the spectra of all samples, with exception of the spectra of sample S#5, is a non-identified emission band with peak around 3.4 eV. Emission bands with similar peak position have been observed in *a*-plane GaN layers and attributed to stacking faults [18,19]. However, a similar value of emission band peak position is not sufficient to provide defect identification and a detailed study will be necessary to achieve correct defect identification. Note that the emission band assigned to the recombination processes involving shallow-acceptors and shallow-donors with no-phonon line at 3.27 eV is not present in these spectra. Higher resolution spectra covering the spectral range between 3.32 and 3.54 eV are represented in Fig. 4b. The spectra of samples S#1, S#4, and S#5 show emission lines related to recombination processes involving the ground state of the free-exciton B (FX_B), the ground state and the first excited state of the free-exciton A (FX_A and FX_A^1, respectively), and the dominant line related to excitons bound to neutral donors ($D^\circ X$, or $O^\circ X$, and $Si^\circ X$) [15]. Around 3.45 eV we detect the so-called two-electron satellite (2ES) spectrum resulting from the recombination processes that leave neutral donors in an excited state after the exciton annihilation. Spectral separations between $D^\circ X$ and 2ES lines yield the intra-center transition energies of the impurities. Fig. 4c depicts the highest resolution spectrum of sample S#1, which illustrates the spectral separation of the recombination processes involving the annihilation of excitons

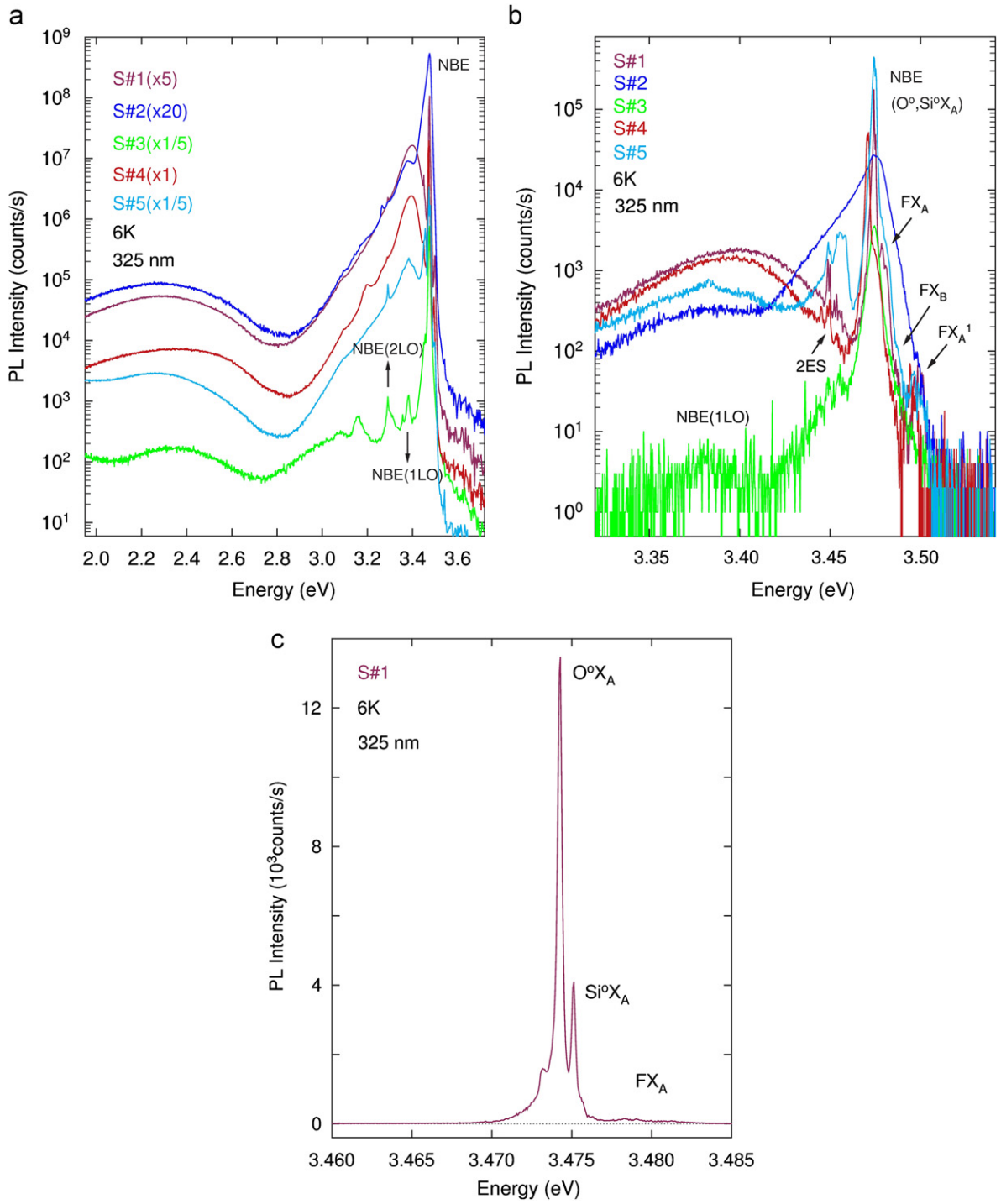

Fig. 4. (a) 5 K PL spectra, measured at low resolution, of thick freestanding GaN samples. (b) 5 K PL spectra, measured at higher resolution of the five samples represented in (a) and (c). 5 K PL spectrum of sample S#1 highlighting the spectral separation between Si and O donor-bound exciton lines.

bound to shallow neutral Si and O donors. The line assigned to the exciton bound to Si donors (Si°X at 3.4751 eV, FWHM ≈ 310 μeV) is less intense than that assigned to the exciton bound to the shallow O donors (O°X at 3.4743, FWHM ≈ 340 μeV), which is consistent with a lower background Si concentration, in agreement with the SIMS analysis [20]. Increase in the concentration of Si and O donors results in a rapid broadening of the FWHM of the Si°X and O°X, resulting in an unresolved, relatively broad D°X line (e.g., spectrum of S#2, in Fig. 4b.). Note that the line shape broadening highlighted in Fig. 4b is consistent with the SIMS results represented in Table 1.

To obtain additional information of the concentration and type of free carries in the thick GaN substrates EPR spectra were obtained at 15 K. Measurements acquired in the dark for three samples with the applied magnetic field parallel to the *c*-axis are shown in Fig. 5. In all cases a single Lorentzian line with *g*-value of ~1.95 is found and has been firmly established as a "fingerprint" of shallow donors/conduction electrons in GaN from previous studies [8]. Due to the absence of resolved electron-nuclear hyperfine structure it is not possible to associate this EPR feature with Si or O impurities that are well-known sources of n-type conductivity in GaN, and verified by high resolution PL

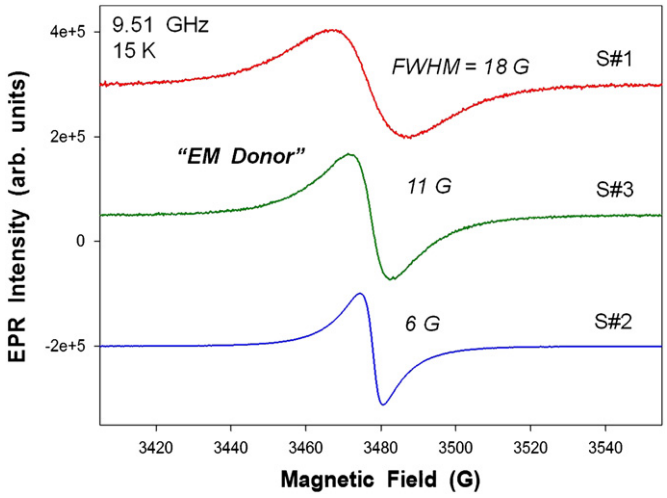

Fig. 5. EPR spectra obtained at 15 K for three representative bulk GaN samples with $\mathbf{B} \| c$-axis.

spectroscopy (Fig. 4c). However, as seen in Table 1, the SIMS measurements clearly indicate that oxygen is roughly one order of magnitude higher in concentration relative to Si in all but one of the samples investigated in this work and, thus, is likely responsible for the largest fraction of the shallow donor EPR signals. Finally, a clear trend observed from the EPR characterization is the decreasing FWHM value of the line width for samples with larger (uncompensated) shallow donor concentration. For example, as shown in Fig. 5, the EPR line width reduction is a factor of three between HVPE GaN samples S#1 and S#2. This so-called "motional narrowing" behavior reflects the averaging out of the electron–nuclear hyperfine interaction between the donor electron spin and the nuclei of the host lattice atoms as reported from previous EPR studies of epitaxial and bulk GaN [8,9]. We note that the observation of the smallest EPR shallow donor line width for sample S#2 is consistent with the SIMS measurements that revealed the highest total concentration of residual O+Si impurities among these five samples.

4. Conclusion

X-ray diffraction studies of several thick, freestanding bulk GaN substrates grown by HVPE are consistent with low densities of edge and screw dislocations and suggest that the natural cleavage plane for this material is the *m*-plane. The sharpness and energy position of the first order Raman scattering spectra of these samples indicate that high quality crystals with relatively low free-carrier concentrations have been accomplished. The small intensity and line width of the lines associated with recombination processes involving the annihilation of excitons bound to neutral shallow donors and the small intensity of the deep emission bands related to compensation centers is consistent with low free-carrier concentration and relatively low compensation levels. These observations were verified by EPR experiments and are consistent with the relatively low level of impurities detected by SIMS. These results clearly indicate that if the oxygen background impurity concentration can be reduced to the level achieved for Si, GaN substrates growth by HVPE techniques could be conveniently used for high-frequency, high-power switches.

References

[1] J.A. Freitas Jr., M. Gowda, J.G. Tischler, J.-H. Kim, L. Liu, D. Hanser, Journal of Crystal Growth 310 (2008) 3968.
[2] J.A. Freitas Jr., M.A. Mastro, E.A. Imhoff, M.J. Tadjer, C.R. Eddy, F.J. Kub, Journal of Crystal Growth 312 (2010) 2616.
[3] B.S. Kang, F. Ren, Y. Irokawa, K.W. Baik, S.J. Pearton, C.-C. Pan, G.-T. Chen, J.-J. Chyi, H.-J. Ko, H.-Y. Lee, Journal of Vacuum Science and Technology B 22 (2004) 710.
[4] K. Maier, M. Kunzer, U. Kaufmann, J. Schneider, B. Monemar, I. Akasaki, H. Amano, Materials Science Forum 143–147 (1994) 93.
[5] P.G. Baranov, I.V. Ilyin, E.N. Mokhov, Solid State Communications 101 (1997) 611.
[6] K.H. Chow, G.D. Watkins, A. Usui, M. Mizuta, Physical Review Letters 85 (2000) 2761.
[7] N.T. Son, C.G. Hemmingsson, T. Paskova, K.R. Evans, A. Usui, N. Morishita, T. Ohshima, J. Isoya, B. Monemar, E. Janzén, Physical Review B 80 (2009) 153202.
[8] W.E. Carlos, J.A. Freitas Jr., M. Asif Khan, D.T. Olson, J.N. Kuznia, Physical Review B 48 (1993) 17878 and references therein.
[9] E.R. Glaser, W.E. Carlos, G.C.B. Braga, J.A. Freitas Jr., W.J. Moore, B.V. Shanabrook, R.L. Henry, A.E. Wickenden, D.D. Koleske, Physical Review B 65 (2002) 085312 and references therein.
[10] M.A. Moran, M.E. Vickers, Reports on Progress in Physics 72 (2009) 036502.
[11] S.R. Lee, A.M. West, A.A. Allerman, K.E. Waldrip, D.M. Follstaedt, P.P. Provencio, D.D. Koleske, C.R. Abernathy, Applied Physics Letters 86 (2005) 241904.
[12] L. Bergman, M. Dutta, R.J. Nemanich, Raman Scattering Spectroscopy and Analyses of III–V Nitride Based Materials, Raman Scattering in Material, Springer, Berlin, 2000 Chapter 7.
[13] P. Perlin, J. Camassel, W. Knap, T. Taliercio, J.C. Chervin, T. Suski, I. Grzegory, S. Porowski, Applied Physics Letters 67 (1995) 2524.
[14] L. Bergman, D.A. Alexson, P.L. Murphy, R.J. Nemanich, M. Dutta, M.A. Stroscio, C. Balkas, H. Shin, R.F. Davis, Physical Review B 59 (20) (1999) 12977–12982.
[15] J.A. Freitas Jr., W.J. Moore, B.V. Shanabrook, G.C.B. Braga, S.K. Lee, S.S. Park, J.Y. Han, Physical Review B 66 (2002) 233311.
[16] D.S. Green, U.K. Mishra, J.S. Speck, Journal of Applied Physics 95 (2004) 8456.
[17] A.E. Wickenden, D.D. Koleske, R.L. Henry, R.J. Gorman, M.E. Twigg, M. Fatemi, J.A. Freitas Jr., W.J. Moore, Journal of Electronic Materials 29 (21) (2000) R114.
[18] R. Liu, A. Bell, F.A. Ponce, C.Q. Chen, J.W. Yang, M.A. Khan, Applied Physics Letters 86 (2005) 021908.
[19] P.P. Paskov, R. Schifano, B. Monemar, T. Paskova, S. Figge, D. Hommel, Journalof Applied Physics 98 (2005) 093519.
[20] M. Murthy, J.A. Freitas Jr., J. Kim, E.R. Glaser, D. Storm, Journal of Crystal Growth 305 (2007) 393.